Chinese Chemical Letters 32 (2021) 3469–3473

Contents lists available at ScienceDirect

Chinese Chemical Letters

journal homepage: www.elsevier.com/locate/cclet

Communication

Eco-friendly non-acid intercalation and exfoliation of graphite to graphene nanosheets in the binary-peroxidant system for EMI shielding

Ping Wang[a,b], Bin Guo[a], Zhi Zhang[a], Weinan Gao[a], Wei Zhou[a], Huaxin Ma[a], Wenyu Wu[a], Junfeng Han[b,*], Ruijun Zhang[a,*]

[a] State Key Laboratory of Metastable Materials Science and Technology, Yanshan University, Qinhuangdao 066004, China
[b] Key Laboratory of Advanced Optoelectronic Quantum Architecture and Measurement, Ministry of Education, School of Physics, Beijing Institute of Technology, Beijing 100081, China

ARTICLE INFO

Article history:
Received 13 January 2021
Revised 20 March 2021
Accepted 28 May 2021
Available online 1 June 2021

Keywords:
Graphene exfoliation
Eco-friendly
Graphene paper
EMI shielding

ABSTRACT

The development of the preparation strategy for high-quality and large-size graphene *via* eco-friendly routes is still a challenging issue. Herein, we have successfully developed a novel route to chemically exfoliate natural graphite into high-quality and large-size graphene in a binary-peroxidant system. This system is composed of urea peroxide ($CO(NH_2)_2 \cdot H_2O_2$) and hydrogen peroxide (H_2O_2), where $CO(NH_2)_2 \cdot H_2O_2$ is used in preparing graphene for the first time. Benefiting from the complete decomposition of $CO(NH_2)_2 \cdot H_2O_2$ and H_2O_2 into gaseous species under microwave (MW) irradiation, no water-washing and effluent-treatment are needed in this chemical exfoliation procedure, thus the preparation of graphene in an eco-friendly way is realized. The resultant graphene behaves a large-size, high-quality and few-layer feature with a yield of ~100%. Then 4 μm-thick ultrathin graphene paper fabricated from the as-exfoliated graphene is used as an electromagnetic interference (EMI) shielding material. And its absolute effectiveness of EMI shielding (SSE/t) is up to 34,176.9 dB cm^2/g, which is, to the best of our knowledge, among the highest values so far reported for typical EMI shielding materials. The EMI shielding performance demonstrates a great application potential of graphene paper in meeting the ever-increasingly EMI shielding demands in miniaturized electronic devices.

Due to the unique properties of graphene, it exhibits great application potential in thermal and conductive polymer composite films, smart electronics and portable devices, mechanical and structural reinforcement and so forth [1-3]. Obviously, the development of facile and efficient preparation technologies of graphene is a critical prerequisite for its industrial applications.

Up to date, varieties of preparation methods exfoliating graphite into graphene have been developed. Among them, the oxidation–reduction route is widely used. However, the usage of strong oxidants and strong acids leads to the inferior quality of the as-prepared graphene and the environmentally detrimental impact caused by the effluent like waste acids [4,5]. In contrast, mechanical exfoliation of graphite into graphene seems more eco-friendly, since this kind of techniques do not involve the usage of strong oxidants or strong acids [6-10]. However, graphite would break into little fragments during the graphene preparation, so the as-obtained flakes of graphene are very small in size, which hinders its further applications. In a word, how to prepare the high-quality and large-size graphene *via* an eco-friendly route is still a challenging issue and further investigation is required.

Herein, we have proposed a novel non-acid preparation strategy of graphite to the high-quality and large-size graphene, which is realized by chemically intercalating and exfoliating graphite in a binary-peroxidant system followed by microwave (MW) irradiation. The newly-developed binary system is comprised of urea peroxide ($CO(NH_2)_2 \cdot H_2O_2$) and hydrogen peroxide (H_2O_2). Where $CO(NH_2)_2 \cdot H_2O_2$ is used in graphene preparation for the first time. Since the used peroxidants-$CO(NH_2)_2 \cdot H_2O_2$ and H_2O_2 can be completely decomposed into gaseous species under microwave (MW) irradiation, no water-washing and effluent-treatment are needed during the whole process of graphene preparation. Thereby the eco-friendly way of graphene preparation is guaranteed. The as-exfoliated graphene behaves large-size, high-quality and few-layer

* Corresponding authors.
E-mail addresses: pkuhjf@bit.edu.cn (J. Han), zhangrj@ysu.edu.cn (R. Zhang).

https://doi.org/10.1016/j.cclet.2021.05.064
1001-8417/

features with a yield of ~100%. Furthermore, the ultrathin graphene film (only ~ 4 μm in thickness) has been fabricated by simple vacuum filtration from the obtained graphene solution without any high-temperature treatment. Which has shown excellent electrical conductivity and electromagnetic interference (EMI) shielding performance, suggesting its great potential in satisfying the increasing needs for EMI shielding in electronic devices.

Firstly, we investigated the feasibility of exfoliating natural graphite (NG) into graphene in a single-peroxidant system followed by MW irradiation. NG powders were soaked in a single peroxidant saturated solution followed by 500 W MW irradiation, the as-treated products was then collected for further assessment. Fig. S1 (Supporting information) shows the volumetric comparison of the used pristine NG powders and the product obtained in $(NH_4)_2S_2O_8$, $Na_2CO_3\cdot H_2O_2$ and $CO(NH_2)_2\cdot H_2O_2$ system, respectively. Clearly, there is no obvious difference in volume between NG and these obtained products. However, the further field emission scanning electron microscope (FESEM) observation discovered that some curled-up and loose structures were formed in all the products obtained in these single-peroxidant system, as displayed in Fig. S2 (Supporting information). This demonstrates that the exfoliation from graphite to graphene aggregates (GAs) happened after the soaking of NG powders in a single peroxidant system and subsequent MW irradiation.

Unfortunately, we found that only a small number of NG powders had been exfoliated into GAs, implying a poor exfoliation yield. Indeed, the aqueous solution of peroxidant ($(NH_4)_2S_2O_8$, $Na_2CO_3\cdot H_2O_2$ and $CO(NH_2)_2\cdot H_2O_2$) has the properties of H_2O_2, which can release oxygen in the water. When graphite powders were soaked in peroxidant aqueous solution followed by 500 W MW irradiation, however, there was no obvious difference in volume between the pristine graphite and the obtained product. And only a small number of graphite powders had been exfoliated into GAs, implying that only a few graphite flakes were intercalated and exfoliated. Since the edge-oxidizing is the important prerequisite for the intercalation of graphite, the fact that only a small number of graphite powders were exfoliated into GAs suggests the oxidization of few graphite edges in the peroxidant aqueous solution. That is to say, although there H_2O_2 existed in the peroxidant ($(NH_4)_2S_2O_8$, $Na_2CO_3\cdot H_2O_2$ and $CO(NH_2)_2\cdot H_2O_2$) aqueous solution, the concertation of H_2O_2 is not enough to oxidize many graphite edges. To increase the concertation of H_2O_2 in the peroxidant saturated solution thus enhance the edge-oxidization of graphite, H_2O_2 (30%) solution was used to replace the water solvent. Three binary-peroxidant systems were further developed (*i.e.*, $(NH_4)_2S_2O_8/H_2O_2$, $Na_2CO_3\cdot H_2O_2/H_2O_2$ and $CO(NH_2)_2\cdot H_2O_2/H_2O_2$) respectively. Interestingly, after soaking NG powders in one of the above binary-peroxidant system followed by 500 W MW irradiation, we found the obvious volumetric expansion of collected products compared with that of pristine NG powders (Figs. 1a-c). Further characterization confirmed that a lot of loosely worm-like GAs were formed and only a small amount of un-exfoliated NG flakes were remained in all these products. From this, the GAs yield can be roughly deduced as 30%, 30% and 70% for the $(NH_4)_2S_2O_8/H_2O_2$, $Na_2CO_3\cdot H_2O_2/H_2O_2$ and $CO(NH_2)_2\cdot H_2O_2/H_2O_2$ system, respectively. Figs. 1d-f provide the FESEM images of the typical GAs obtained in the three binary-peroxidant systems, which all show the well-exfoliated structures with a semi-transparent feature.

Although graphite can be exfoliated into more GAs after graphite powders were soaked in $CO(NH_2)_2\cdot H_2O_2/H_2O_2$ system at room temperature followed by 500 W MW irradiation, the GAs yield of $< 100\%$ is still not satisfied. Since the peroxidant can behave stronger oxidability at higher temperature [11], the soaking experiments at different temperatures (30, 45, 60, 75 and 90 °C) were performed to achieve a higher yield of GAs by strengthening

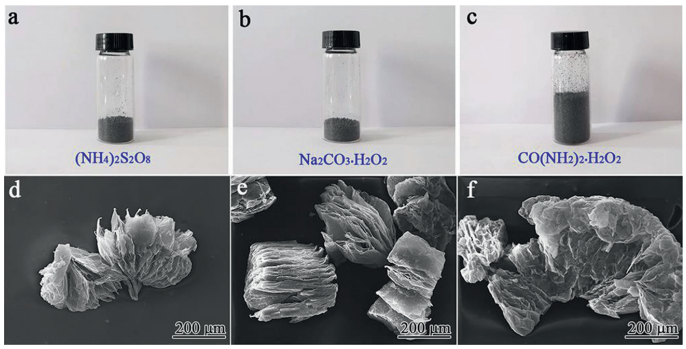

Fig. 1. Volumetric comparison of the product obtained in (a) $(NH_4)_2S_2O_8/H_2O_2$, (b)$Na_2CO_3\cdot H_2O_2/H_2O_2$ and (c) $CO(NH_2)_2\cdot H_2O_2/H_2O_2$ system; the corresponding FESEM images of the GAs obtained in (d) $(NH_4)_2S_2O_8/H_2O_2$ system, (e) $Na_2CO_3\cdot H_2O_2/H_2O_2$ system and (f) $CO(NH_2)_2\cdot H_2O_2/H_2O_2$ system.

the oxidization of the graphite edges. We have found that when the soaking is performed at 60 °C, graphite (Fig. S3 in Supporting information) can be exfoliated into ~100% GAs after the MW irradiation, as displayed in Fig. S4 (Supporting information). This result suggests that, the soaking temperature of 60 °C is the most feasible in this binary system.

To thoroughly investigate the effect of H_2O_2 on the chemical exfoliation of graphite, three comparative experiments were designed and performed by soaking the graphite sample in $CO(NH_2)_2\cdot H_2O_2$, H_2O_2 and $CO(NH_2)_2\cdot H_2O_2 + H_2O_2$ at 60 °C, respectively. The three soaked graphite samples were characterized by X-ray diffraction, as shown in Fig. S5 (Supporting information). It can be observed that two strong X-ray diffraction peaks on the pattern of pristine graphite are located at 26.7° and 54.8° in Fig. S5a, corresponding to (002) and (004) crystal planes, respectively. It is worth noting that both the $CO(NH_2)_2\cdot H_2O_2$-soaked (Fig. S5b) and H_2O_2-soaked (Fig. S5c) graphite samples exhibit a similar X-ray diffraction (XRD) pattern with the pristine graphite, indicating no obvious structural change when the graphite is soaked in the single peroxidant ($CO(NH_2)_2\cdot H_2O_2$ or H_2O_2) system. As for the $CO(NH_2)_2\cdot H_2O_2 + H_2O_2$-soaked graphite samples, its XRD pattern (Fig. S5d) is distinctly different. Beside the (002) and (004) graphite peaks, four additional diffraction peaks appeared at 10.2°, 19.1°, 25.9° and 29.1°, corresponding to (002), (004), (005) and (006) planes, respectively. This result implies the formation of graphite intercalation compound (GIC) in this $CO(NH_2)_2\cdot H_2O_2 + H_2O_2$-soaked graphite sample [12]. Based on the XRD characterization above, therefore, we can conclude that the introduction of H_2O_2 in the $CO(NH_2)_2\cdot H_2O_2$ system can enhance the opening of the graphite edge, thus facilitating the intercalation of graphite. Due to the thermal instability, the intercalated $CO(NH_2)_2\cdot H_2O_2$ and H_2O_2 will then decompose into gaseous substances under MW irradiation, leading to a sudden pressure raise between interlayer gallery of graphite. Once the sudden raise of gas pressure can overcome the Van der Waals force, GICs will be transformed into GAs. Fig. 2 provides a schematic of the intercalation and exfoliation of graphite to graphene *via* the optimized route.

The GAs prepared by the optimized exfoliation route were dispersed into ethanol under 100 W ultrasonication for 20 min, and a graphene dispersion was acquired. FESEM and high resolution transmission electron microscope (HRTEM) were performed to determine the morphologies of the product. Fig. 3a displays FESEM image of some graphene nanosheets extracted randomly from the dispersion, which are restacked but exhibit a crumpled and wrinkled structural feature. Furthermore, in order to avoid this restacking, the obtained graphene dispersion was deposited on

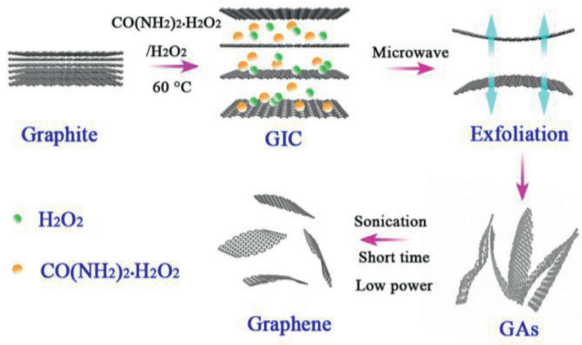

Fig. 2. Schematic of the intercalation and exfoliation of graphite to graphene *via* the optimized route.

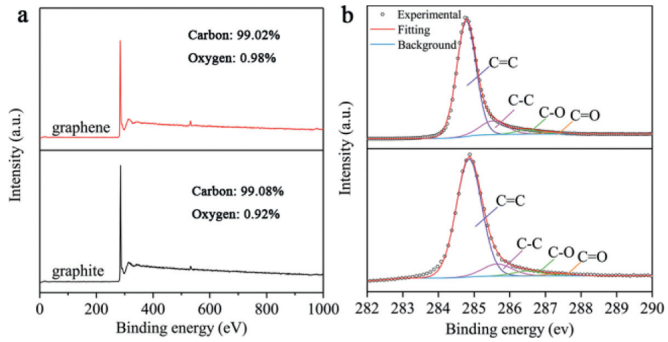

Fig. 4. (a) XPS survey spectra of graphite and graphene; (b) C 1s spectra of graphite and graphene.

a Cu micro-grid for FESEM and HRTEM characterization to measure the areal size and layered number of graphene nanosheets more clearly. FESEM observation shows that the Cu frame is clearly visible through the crumpled and wrinkled graphene nanosheets (Fig. 3b), suggesting a semi-transparent feature for the graphene. This level of transparency implies that the obtained graphene has a few layers feature [13]. By measuring 40 graphene nanosheets under FESEM observation, their areal size distribution histogram is plotted in Fig. 3c, from which the average areal size of graphene nanosheets is calculated to be ~160 um^2, far larger than those acquired by other eco-friendly exfoliation methods reported previously [6-9]. Fig. 3d shows representative TEM image of graphene with crumpled morphology, the folded and scrolled edge was regarded as intrinsic property of graphene nanosheets. The edge stripes of wrinkle nanosheet in HRTEM image revealed that the as-prepared graphene was 6 layers (the inset in Fig. 3d). Atomic force microscopy (AFM) height profile analysis was further employed to assess the thickness of graphene nanosheets. Fig. 3e displays a typical AFM image of the exfoliated graphene, it can be determined that the thickness of nanosheet was approximately 3.8 nm. Furthermore, a histogram of the thickness distribution based on the statistical analysis for 40 graphene nanosheets is showed in Fig. 3f, which enables us to identify the average thickness of the as-exfoliated graphene sheet is ~4 nm, corresponding to ~6 layers [14], which is consistent with HRTEM characterization.

Furthermore, X-ray photoelectron spectroscopy (XPS) measurement was employed to examine defects and functional groups of the as-exfoliated graphene nanosheets, as displayed in Fig. 4. The XPS survey spectrum (Fig. 4a) of the graphene nanosheets shows a prominent C1s peak at 284.8 eV and a weak O 1s peak at 532.2 eV, respectively. The calculated O content of the graphene is only 0.98%, a little higher than that of NG (0.92%) but far lower than those of the graphene obtained by other conventional chemical exfoliation methods [15,16]. Fig. 4b shows the typical C 1s core level spectra of graphite and graphene nanosheets. Both the C 1s spectra could be fitted with four different components with binding energy at 284.8 eV, 285.6 eV, 286.6 eV and 287.2 eV, assigned to C=C, C-C, C-O and C=O bonds, respectively[16]. This result demonstrates that the existence of similar oxygen species in natural graphite and as-exfoliated graphene nanosheets. This should be ascribed to the use of MW irradiation in this work. Generally, MW irradiation is employed as a convenient and rapid heating source. However, it was discovered that MW-irradiation can effectively reduce the graphene oxide [17], heating treatment can repair the nano-holes and recover the high-quality graphene conjugated network [18-20]. Therefore, although the peroxidants can oxidize the pristine

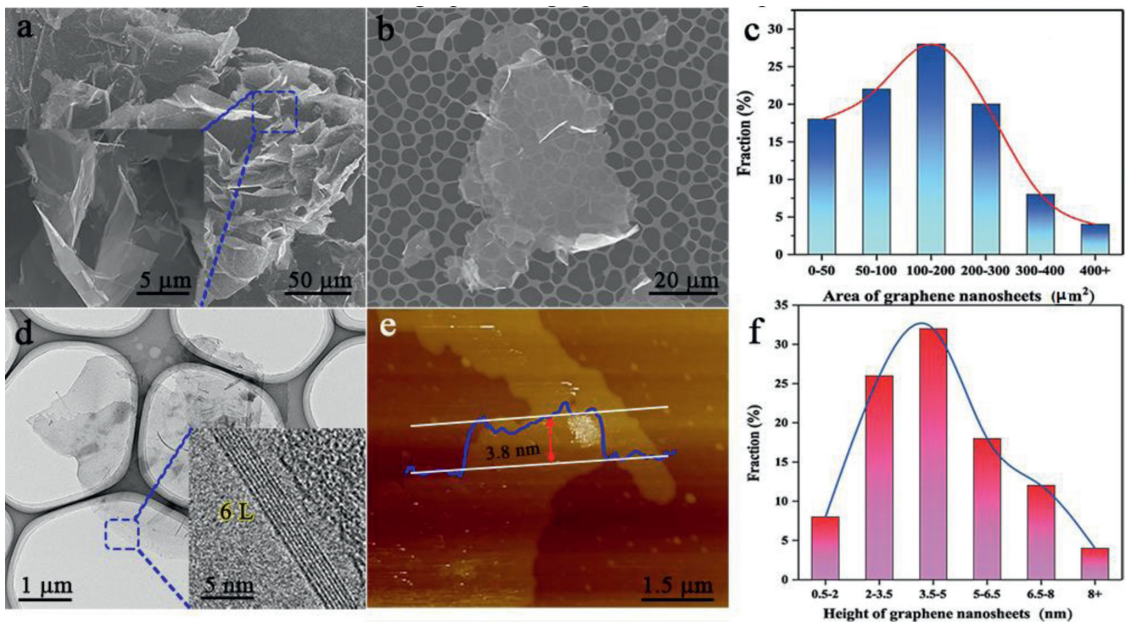

Fig. 3. (a, b) FESEM images of the exfoliated graphene nanosheets and (c) histogram of the areal size distribution observed from 40 nanosheets. (d) Representative TEM and HRTEM images of graphene. (e) AFM image of the exfoliated graphene nanosheets and (f) histogram of the thickness distribution calculated from 40 nanosheets.

graphite leading to the increase of O content on the graphite, this O increment could be removed during the MW-irradiation. In consideration of the low O content and the unchanged oxygen species existing in the obtained graphene, we can deduce that the chemical exfoliation in the $CO(NH_2)_2 \cdot H_2O_2/H_2O_2$ system has very weak impact on the structure of graphite, thus ensuring the high-quality of graphene.

Raman spectroscopy is a widely applied technique to evaluate the quality and thickness of as-exfoliated graphene nanosheets. As displayed in Fig. S6 (Supporting information), two sharp peaks attributed to G band (~1580 cm^{-1}) and 2D band (~2700 cm^{-1}) respectively on the spectra of the resultant graphene and pristine graphite, confirming both the samples were highly crystallized. Meanwhile, both the samples existed a very weak D band (1350 cm^{-1}), resulting from the existence of defects such as edges or structural disorders [21]. It should be noted that the D/G band intensity ratio (I_D/I_G) can provide a measurement of the degree of structural defects. The calculated I_D/I_G ratio of graphite (0.05) and graphene (0.07) were similar, indicating that this chemical exfoliation could avoid most fragmentation of graphene nanosheets [22]. Moreover, based on the Raman peak redshift (from 2717 cm^{-1} to 2704 cm^{-1}) and the shape of 2D band, these results revealed few-layer feature of the obtained graphene nanosheets [21].

To further identify surface functional groups on graphite, graphite and as-exfoliated graphene were tested through Fourier transform infrared spectroscopy (FTIR) analysis in Fig. S7 (Supporting information). It can be observed that three absorption bands around 1400 cm^{-1}, 1630 cm^{-1} and 3400 cm^{-1} were presented in the FTIR spectrum of graphite and as-exfoliated graphene, which were assigned to C–O group, C=O group and −OH group, respectively [23]. The FTIR spectrum of graphite and as-exfoliated graphene had no significant difference, indicating that both samples had very similar chemical groups, which is consistent with XPS results.

X-ray diffraction was used to investigate the crystal structure of the as-exfoliated graphene nanosheets, as shown in Fig. S8 (Supporting information). Obviously, a sharp and strong X-ray diffraction signals at 26.7° was attributed to the typical characteristic of graphite with high crystalline, corresponding to (002) plane. After exfoliating in the $CO(NH_2)_2 \cdot H_2O_2/H_2O_2$ system, the product exhibited a weak and flat (002) peak with broad full width, this is attributed to the exfoliated yet restacked state of the graphene powder [16]. No new peaks for graphene oxide appeared, suggesting graphite structure has not been oxidized in the $CO(NH_2)_2 \cdot H_2O_2/H_2O_2$ system followed by MW irradiation.

To conclude, we have developed a novel chemical exfoliation system of graphite, where graphite powders can completely exfoliated into GAs through soaking in the $CO(NH_2)_2 \cdot H_2O_2/H_2O_2$ system followed by MW irradiation. The resultant graphene nanosheets, obtained from GAs by simple low-power sonication, behave a large-sized and high-quality feature. Distinctly from those conventional chemical exfoliation methods, our exfoliation route does not involve the usage of corrosive acids. In the meantime, benefiting from the decomposition of the used peroxidants under MW irradiation, no water-washing and effluent-treatment are required during the whole graphene preparation process. This suggests that our technical strategy is outstanding in exfoliating the large-size and high-quality graphene nanosheets based on eco-friendly notion.

To explore the possible application of the as-exfoliated graphene nanosheets, a silver-gray graphene paper (GP) was prepared from graphene dispersion by simple vacuum filtration and room-temperature mechanical pressing, as displayed in Fig. 5a. The GP sample can be tightly rolled and deeply folded like paper in the life (Fig. 5b and Fig. S9 in Supporting information), the visible creases was observed in the opened GP but without any crack or fracture, suggesting that the obtained GP is superior in toughness. As expected, benefiting from the large lateral size and high quality of the as-exfoliated graphene nanosheets, the fabricated GP with ~4 μm (Fig. 5c) behaves an excellent electrical performance, its average electrical conductivity is up to 6.1 × 10^5 S/m. Fig. 5c discloses that the graphene nanosheets are well aligned in the GP. This well-aligned layered architecture together with the high electrical conductivity should suggest its great potential in EMI shielding [24]. Therefore, we performed the measurement of EMI SE for the GP in the X-band range (8.2–12.4 GHz) by a Vector Network Analyzer. As expected, the ~1 μm-thick and ~4 μm-thick GP exhibits a superior EMI SE value of 32 dB and 43 dB, respectively (Fig. 5d and Fig. S10 in Supporting information). By comparing SE_{abs} and SE_{ref} value of ~1.0 μm and ~ 4 μm-thick GP samples at a constant frequency of 8.2 GHz, it can be known that SE_{abs} has more contribution to the SE_{total} value for the ~ 4 μm-thick GP sample. Which indicates that the shielding due to absorption is the crucial factor in determining the EMI performance with the increasing of the GP thickness.

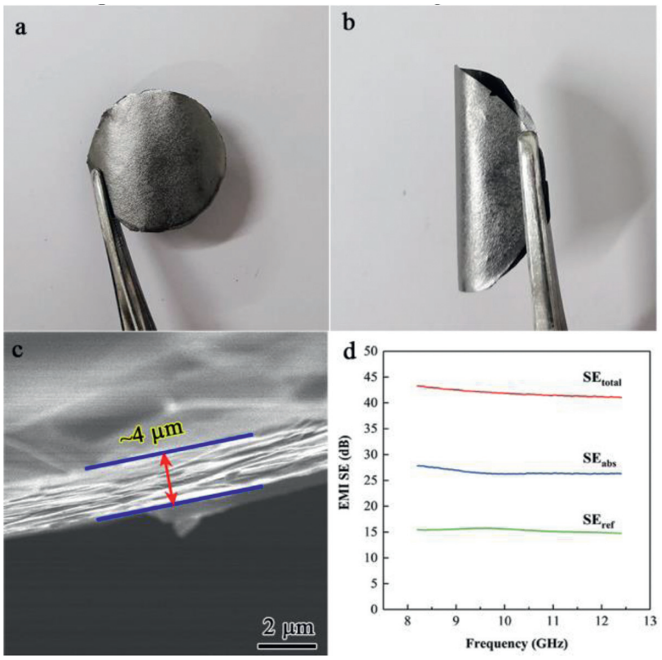

Fig. 5. (a) The fabricated GP, (b) the deeply rolled GP, (c) the cross-sectional SEM image of GP, which exhibits a well-aligned layered structure. (d) EMI shielding performance of GP.

Now the miniaturization of electronic devices has become an inevitable trend with the development of electronic technology. Particularly for EMI shielding application, the ultra-thin EMI shielding materials having a high EMI Shielding effectiveness are urgently needed. In this situation, the absolute effectiveness of EMI shielding (SSE/t) is of more practical value to assess the shielding performance of materials [25]. It is known that the SSE/t value can be obtained by dividing SE with density (ρ) and thickness (t). Therefore, the SSE/t value of the fabricated GP is calculated as 34,176.9 dB cm^2/g, which is higher than mostly typical EMI shielding materials reported previously (Fig. S11 in Supporting information) [24,26-37]. Based on this, we can conclude that this ultrathin GP will be of great advantage in satisfying the ever-growingly EMI shielding requirement of miniaturized electronic devices.

In this work, an attempt has been made to investigate the feasibility of chemically exfoliating natural graphite into graphene in a non-acid system. On the basis of understanding on the exfoliation of graphite in a single-peroxidant system, we have successfully developed a novel non-acid preparation strategy of

graphite to the high-quality and large-size graphene, which is realized by chemically intercalating and exfoliating graphite in the $CO(NH_2)_2 \cdot H_2O_2/H_2O_2$ system followed by MW irradiation. Due to the complete decomposition of $CO(NH_2)_2 \cdot H_2O_2$ and H_2O_2 into gaseous species under MW irradiation, no water-washing and effluent-treatment are required during the whole chemical exfoliation, thereby ensuring the realization of preparing graphene in a eco-friendly way. The as-exfoliated graphene behaves a few-layer feature with a yield of ~100%. Interestingly, the ~4 μm-thick ultrathin graphene paper, fabricated by simple vacuum filtration from the obtained graphene solution with no high-temperature treatment, exhibits excellent EMI shielding performance. Its SSE/*t* value is higher than most typical EMI shielding materials reported previously, suggesting its great potential in satisfying the increasing needs for EMI shielding in miniaturized electronic devices.

Declaration of competing interest

The authors declare that they have no known competing financial interests or personal relationships that could have appeared to influence the work reported in this paper.

Acknowledgments

The study was supported by National Natural Science Foundation of China (No. 51872253) and supported by Hebei Natural Science Foundation of China (No. E2019203480).

Supplementary materials

Supplementary material associated with this article can be found, in the online version, at doi:10.1016/j.cclet.2021.05.064.

References

[1] Z. Tang, H. Kang, Z. Shen, et al., Macromolecules 45 (2012) 3444–3451.
[2] Z. Hao, Y. Pan, W. Shao, Q. Lin, X. Zhao, Biosens. Bioelectron. 134 (2019) 16–23.
[3] S. Ng, N. Noor, Z. Zheng, NPG Asia Mater. 10 (2018) 217–237.
[4] X. Wang, A. Narita, K. Müllen, Nat. Rev. Chem. 2 (2018) 1–10.
[5] X. Chen, W. Li, D. Luo, et al., ACS Nano 11 (2017) 665–674.
[6] A. Yoshihiko, D.T. Jonathon, K. Masatoshi, et al., Carbon 142 (2019) 261–268.
[7] J.G. Viviana, M.R. Antonio, L. Verónica, et al., Green Chem. 20 (2018) 3581–3592.
[8] K. Chen, W. Zhang, X. Pan, et al., Inorg. Chem. 57 (2018) 5560–5566.
[9] J. Kim, S. Kwon, D. Cho, et al., Nat. Commun. 6 (2015) 8294.
[10] T. Lin, J. Chen, H. Bi, et al., J. Mater. Chem. A 1 (2013) 500–504.
[11] J. Kronholm, M.L. Riekkola, Environ. Sci. Technol. 33 (1999) 2095–2099.
[12] F.Y. Kang, Y. Leng, T.Y. Zhang, J. Phys. Chem. Solids 57 (1996) 889–892.
[13] D. Ayrat, V.K. Dmitry, S. Alexander, et al., Science 331 (2011) 1168–1172.
[14] Z. Cheng, Q. Zhou, C. Wang, Q. Li, C. Wang, Nano Lett. 11 (2011) 767–771.
[15] S. Lin, L. Dong, J. Zhang, H. Lu, Chem. Mater. 28 (2016) 2138–2146.
[16] P. He, H. Gu, G. Wang, et al., Chem. Mater. 29 (2017) 8578–8582.
[17] R. Jakhar, J.E. Yap, R. Joshi, Carbon 170 (2020) 277–293.
[18] Y. Chen, Y. Wang, S. Zhu, et al., Mater. Today 24 (2019) 26–32.
[19] Y. Chen, K. Fu, S. Zhu, et al., Nano lett. 16 (2016) 3616–3623.
[20] S. Liu, P. Wang, C. Liu, Small 16 (2020) 2002856.
[21] A.C. Ferrari, J.C. Meyer, V. Scardaci, et al., Phys. Rev. Lett. 97 (2006) 187401.
[22] J. Lin, Y. Huang, S. Wang, et al., Ind. Eng. Chem. Res. 56 (2017) 9341–9346.
[23] G. Surekha, K.V. Krishnaiah, N. Ravi, R.P. Suvarna, J. Phys. Conf. Ser. 1495 (2020) 012012.
[24] F. Shahzad, M. Alhabeb, C.B. Hatter, et al., Science 353 (2016) 1137–1140.
[25] J. Zhong, W. Sun, Q. Wei, et al., Nat. Commun. 9 (2018) 3484.
[26] L. Zhang, N.T. Alvarez, M. Zhang, et al., Carbon 82 (2015) 353–359.
[27] B. Shen, Y. Li, D. Yi, et al., Carbon 102 (2016) 154–160.
[28] E. Zhou, J. Xi, Y. Liu, et al., Nanoscale 9 (2017) 18613–18618.
[29] J. Xi, Y. Li, E. Zhou, et al., Carbon 135 (2018) 44–51.
[30] Z. Chen, C. Xu, C. Ma, W. Ren, H. Cheng, Adv. Mater. 25 (2013) 1296–1300.
[31] W. Song, X. Guan, L. Fan, et al., Carbon 93 (2015) 151–160.
[32] X. Sun, X. Liu, X. Shen, et al., Compos. Part. A: Appl. Sci. Manufac. 85 (2016) 199–206.
[33] E. Zhou, J. Xi, Y. Guo, et al., Carbon 133 (2018) 316–322.
[34] Q. Song, F. Ye, X. Yin, et al., Adv. Mater. 29 (2017) 1701583.
[35] S. Lu, J. Shao, K. Ma, et al., Carbon 136 (2018) 387–394.
[36] D. Lu, Z. Mo, B. Liang, et al., Carbon 133 (2018) 457–463.
[37] K. Ji, H. Zhao, J. Zhang, J. Chen, Z. Dai, Appl. Surf. Sci. 311 (2014) 351–356.